Performance comparison of axial-flux switched reluctance machines with non-oriented and grain-oriented electrical steel rotors

Racha Aydoun, Guillaume Parent, Abdelmounaïm Tounzi, Jean-Philippe Lecointe

Research Article

Racha Aydoun, Guillaume Parent, Abdelmounaïm Tounzi, and Jean-Philippe Lecointe*

Performance comparison of axial-flux switched reluctance machines with non-oriented and grain-oriented electrical steel rotors

Abstract: This paper studies the performance of an axial-flux switched reluctance machine (AFSRM) using GOES (grain-oriented electrical steel) in its rotor and comparing it to a NOES (non-oriented electrical steel) rotor. Indeed, the AFSRM structure lends itself well to the use of GOES, especially at the rotor. In order to evaluate the intrinsic capabilities of the AFSRM, self-inductance versus rotor position and static torque were numerically simulated at a given operating point and used as indicators for the NOES and GOES performance comparison. The static torque is also used to determine and compare the torque per volume ratios and grasp the impact of GOES use in a 3D rotating structure. The introduction of GOES in a rotating machine leads to an improvement of the electromagnetic torque mean and maximum values, allowing to evaluate the GOES impact on the machine performance.

Keywords: axial-flux switched reluctance machine, grain-oriented electrical steel, non-oriented electrical steel, electromagnetic torque

1 Introduction

Numerous applications require designing electrical machines with large power-to-weight ratio. The majority of these applications need machines to deliver high torques and operate at large speeds while seeking high efficiency. In this respect, switched reluctance machines (SRM) are good candidates as they are known to operate at high torque or at exceptionally high speeds. They are also known to be robust [1] given the fact that they are magnet-free and have no winding at the rotor [2], which makes them reliable in harsh environments. With these advantages in mind, several studies taking interest in the AFSRM proved that it is often more compact than the radial-flux SRM (RFSRM) [3,4]. Consequently, a growing interest is directed towards AFSRM to deliver compact designs [5,6] and thus introducing these machines to various applications.

In order to increase efficiency, it can be advantageous to introduce high performance materials such as grain-oriented electrical steel (GOES), which offers excellent performance when it comes to permeability, high saturation, flux density, and iron losses [7]. Moreover, the introduction of thin GOES sheets comes with limited iron losses [8], higher levels of permeability, and higher saturation levels compared to conventional NOES. However, the anisotropic nature of such material makes it difficult to be used in electrical rotating machines – aside from segmented circuits – as the performance varies depending on the magnetization direction.

Despite the difficulties related to the integration of GOES in a rotating device, several [9–11] papers focused on its use in common AC rotating machines. The authors of ref. [9] proved that induction machines' efficiency can be improved with the use of GOES in their magnetic circuit. More precisely, they showed this improvement by shifting each lamination by an experimentally determined angle of 90° without segmentation. In order to benefit from the easiest magnetization direction, the flux follows a path going from a lamination to the next adjacent one.

Performances of axial- and radial-flux SRM have been studied and showed that the electromagnetic torque can be improved by up to 21% [12] in comparison with a conventional SRM when GOES is used in their magnetic

* **Corresponding author: Jean-Philippe Lecointe,** Univ. Artois, UR 4025, Laboratoire Systèmes Electrotechniques et Environnement (LSEE), Béthune, F-62400, France, e-mail: jphilippe.lecointe@univ-artois.fr
Racha Aydoun, Guillaume Parent: Univ. Artois, UR 4025, Laboratoire Systèmes Electrotechniques et Environnement (LSEE), Béthune, F-62400, France
Abdelmounaïm Tounzi: Univ. Lille, Centrale Lille, Arts et M ètiers ParisTech, HEI, EA 2697 - L2EP - Laboratoire d'Electrotechnique et d'Electronique de Puissance, 59000, Lille, France

circuit. As far as the use of GOES in RFSRM is concerned, the authors of ref. [13] introduced GOES in both stator and rotor teeth, resulting in an increase of the average electromagnetic torque by 10% compared to a Non-Oriented Electrical Steel (NOES) configuration. The authors of ref. [14] compared a GOES and NOES rotor. The comparison showed a steeper inductance slope for the GOES case, also resulting in a 1.5% increase in efficiency due to a decrease in iron losses.

GOES was also introduced in AFSRM by segmenting it in C-core stator teeth [6] to deal with low inductance ratio. The results showed a 5% improvement in the inductance ratio. Authors of ref. [12] also introduced GOES at the stator and rotor teeth of a 12/8 segmented dual stator AFSRM. The parts of the magnetic circuit using GOES are connected to a retaining disk. Several configurations were numerically analyzed including different shapes and deviation angles between the magnetic flux and the rolling direction (RD) of the GOES, before concluding on one configuration where the stator teeth are clipped onto the stator yoke. This layout shows a 21.4% raise in the electromagnetic torque in comparison with the machine using NOES. This torque improvement comes with an increase in manufacturing complexity.

In this paper, a double stator AFSRM using GOES in the rotor is presented and its performance compared to the same AFSRM with a NOES rotor through 3D numerical simulations. The axial structure and the numerical model used are presented and a comparison of their inductance and static torque is given. An analysis leaning on the flux lines distribution and the flux density will be presented in order to conclude on the GOES impact on the machine performance. The two rotors' comparison showed that the introduction of GOES at the rotor results in a steeper inductance slope, leading to an increase in the electromagnetic torque mean value.

2 Numerical model

2.1 GOES integration in the magnetic circuit

The structure considered is an AFSRM with two external stators and a rotor positioned in the middle as shown in Figure 1. This structure has thermal advantages as it allows faster thermal dissipation by having the copper positioned externally.

In terms of magnetic operation, such a structure allows two distinct flux paths [15]: either a loop through
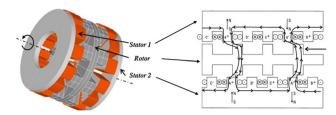

Figure 1: AFSRM and flux path.

the rotor yoke or simply cutting across the rotor as shown in Figure 1. The second flux path configuration is the one considered in our study since it is well-suited for the use of GOES in the rotor with the magnetic flux density only crossing the rotor teeth from a stator to the other.

The GOES is characterized by three typical directions: rolling (RD), transverse (TD), and normal (ND) directions. Thus, by arranging GO sheets such that the RD, which corresponds to the easy magnetization, be in the direction of the magnetic flux of the rotor would increase the variation of the air gap reluctance and thus the performance of the machine.

Furthermore, by using this topology, the rotor yoke is not useful from a magnetic point of view anymore. Therefore, it can be removed and the teeth are individually cut and encapsulated in a nonmagnetic structure.

Previous work ref. [16] has dealt with the study of the contribution of GOES in the case of a configuration close to that of a SRM. Even though the study was mainly conducted in 2D, it has showed that the best improvement in torque mean value happens when GOES is introduced in the magnetic circuit. It would certainly be interesting to introduce the GOES in both the stator and rotor, but given the technological complexity to integrate it in the stator, we have chosen in this study to only introduce GOES at the rotor.

Using this topology, the steel sheets can be arranged in the rotor according to two configurations as shown in both Figures 2 and 3, favoring either the TD or the ND, which may change the saliency:

- Configuration 1 in which a plane is defined by the RD and TD (Figure 2), where TD is in the rotor rotating direction.
- Configuration 2 in which a plane is defined by the RD and the ND (Figure 3), with ND according to the rotating direction.

The anisotropic nature of GOES makes its integration difficult, especially in a machine with a rotating field and the changes in flux path that ensue. Indeed, in a simple and widely used approach, the B(H) curves along the three directions can be considered independant from one another. Therefore, using a identification along each
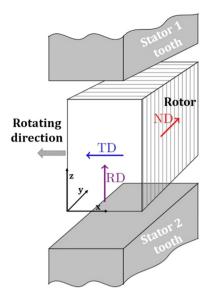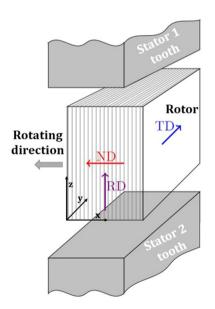
Figure 2: GOES rotor configuration #1.

Figure 3: GOES rotor configuration #2.

Figure 4: NOES and GOES studied characteristics.

of the three axes, it leads to curves such as the ones related to GOES HGO35 shown in Figure 4.

In order to model the anisotropy and analyze the relevant phenomena such as flux distribution and axial device performances, two different types of electrical steel are considered:

- **M400**: Isotropic non-oriented grain electrical steel sheets (0.5 mm thickness);
- **HGO35**: Anisotropic high-grade GOES sheets (0.35 mm thickness) which can be arranged in the different configurations shown in Figures 2 and 3.
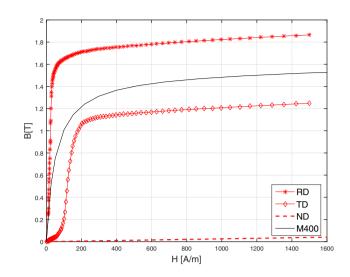
A tensor (equation (1)) is used. Even if this anisotropic model is simple, previous studies (see ref. [11]) showed that it provides acceptable results when it comes to a qualitative study. It is numerically integrated into finite element (FE) simulations and is defined by three main directions: RD, TD, and ND (Figure 4). The relation between magnetic flux density b_i according to each direction and the magnetic field h_i is expressed as follows:

$$\begin{pmatrix} b_{RD} \\ b_{TD} \\ b_{ND} \end{pmatrix} = \begin{pmatrix} \mu_{RD} & 0 & 0 \\ 0 & \mu_{TD} & 0 \\ 0 & 0 & \mu_{ND} \end{pmatrix} \times \begin{pmatrix} h_{RD} \\ h_{TD} \\ h_{ND} \end{pmatrix} \quad (1)$$

In this tensor, μ_i represents each magnetic permeability in the three main directions. In addition to this, permeability in the ND μ_{ND} is considered linear based on the work of ref. [17].

Introducing this tensor represents a simple method allowing the apprehension of the functioning of a rotating machine using GOES, while remaining relevant for drawing conclusions and comparing the machine performances to a conventional NOES case. Because of all the difficulties that come with GOES integration, no comprehensive model for the full behavior of this steel has been put forward to date. In order to quantify the contribution of GOES compared to NOES, the performance of the machine is also determined using M400 characteristic (Figure 4).

2.2 AFSRM 3D model

A double stator 8/6 AFSRM machine is modeled (Figure 5) and studied using the meshing software Gmsh paired
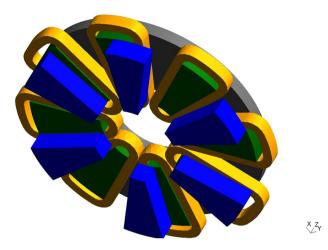
Figure 5: Representation of half of the 3D AFSRM.

Table 1: AFSRM geometric dimensions

Parameters	Name	Value
Stator internal radius [mm]	$R_{s,int}^A$	22.23
Stator external radius [mm]	$R_{s,ext}^A$	59
Rotor internal radius [mm]	$R_{r,int}^A$	22.23
Rotor external radius [mm]	$R_{r,ext}^A$	59
Stator teeth number	N_s	8
Rotor teeth number	N_r	6
Turns number per phase	N_{phase}	520
Stator teeth opening angle [°]	θ_s^A	19.92
Rotor teeth opening angle [°]	θ_r^A	19.975
Shaft radius [mm]	R_a^A	10.5
Airgap thickness [mm]	e^A	0.175

with the free FE solver GetDP. The machine is supplied by injection of a current in the windings and the nonlinear behavior of the magnetic material is taken into account using B–H curve (see Figure 3). The FE simulation is conducted using the magnetostatic vector potential formulation.

Because of symmetry considerations, only half of the machine is shown in Figure 5 (one stator and half a rotor). The rotor teeth are displayed in blue, the stator teeth and yoke in green, and the inductors in yellow. Admittedly, taking advantage of the symmetry would have allowed us to only design a quarter of the machine and thus reduce computation time. However, half of the machine was designed in order to introduce a GOES whose anisotropic characteristics overshadow the machine symmetry.

All the AFSRM geometric dimensions are given in Table 1.

The axial structure lends itself well to the use of GOES in the rotor. In that respect, the trapezoidal-shaped teeth at the rotor will be made up of stacked GOES sheets inserted into a nonmagnetic structure.

Modeling a 3D AFSRM including GOES in its magnetic circuit will lead to fairly heavy calculations. An iterative method is used for the nonlinear resolution and a mesh size adaptation necessary in order to reach a compromise between calculation time and accuracy.

3 Simulation results

In order to compare the performance of the considered AFSRM with NOES and GOES in the rotor teeth, simulations to compute the inductance as a function of rotor position were conducted. Then, a comparison of the resulting electromagnetic torque is presented.

3.1 Inductance comparison

As far as the inductance is concerned, different simulations were conducted for the NOES case and both GOES configurations presented in Figures 2 and 3 for the rated current. Inductance simulations are given for every 5°, and by taking advantage of the symmetry of the inductance curve with respect to rotor position, only positions between the alignment (0°) and the opposition (30°) are simulated. Inductance values for different rotor positions were inferred from the energy value (hereby noted *E*), using the following analytic expression 2:

$$E = \frac{1}{2} \times L \times i^2 \qquad (2)$$

The influence of the anisotropic nature of GOES on the flux path is illustrated in Figure 6 at an intermediate position of 15°. In this figure, only one stator tooth and its opposite rotor tooth are shown. It can be noted that the flux lines tend to generally follow the easy magnetization direction in order to get to the stator tooth. As a result, a flux lines' concentration in the rotor tooth can be observed.

This shows the flux lines cross only through the overlapping effective active surface of iron (Figure 6) and not the entire tooth. The flux lines tend to mainly follow the easy magnetization direction and consequently a straighter marked path in comparison with the conventional case in Figure 7. The same flux path behavior was observed when studying the introduction of GOES in a 2D numerical model [16].

The inductance waveforms results are given in Figure 8 for three different steel cases in the rotor: NOES and two configurations for GOES.

The first outcome that can be noticed from Figure 8 is that the inductance slope is steeper when it comes to both
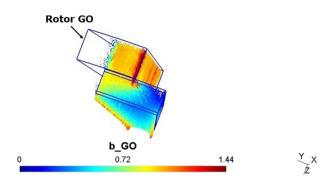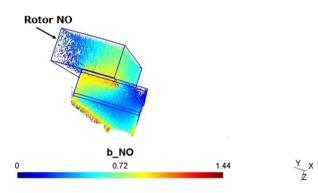
Figure 6: GOES influence on the flux path.

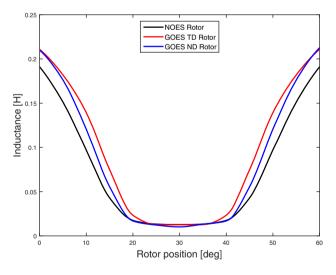**Figure 7:** NOES flux path.

Figure 8: Inductance variation with rotor position.

GOES cases. This result confirms that the use of high permeability GOES improves the inductance slope, with a higher alignment value and a slightly smaller opposite inductance value in comparison with the conventional NOES. The inductance results cover a rotor position range from alignment to opposition, which represents the interest area for the torque production. As we get close to the opposition position, it can be observed that the inductance value difference between GOES and NOES gets smaller. This is quite logical as around these positions, the use of GOES has a minimal impact on the machine performance.

The simulation results also showed that:

- The use of the GOES leads to an increase in alignment inductance value by 10.3% for GOES first configuration (Figure 2) and 9.8% for the second configuration (Figure 3) in comparison with the NOES.

- The second configuration inductance displayed in blue shows a steeper slope on the first half of the curve, i.e., between alignment and 10° rotor position. After an inflection point, the slope becomes smoother between 15° to 25°. The impact of these slope changes on the electromagnetic torque will be analyzed accordingly.

3.2 Electromagnetic torque comparison

The electromagnetic static torque allowing us to evaluate the intrinsic performance of SRM at a given current level is determined based on the energy E and the rotor position θ. Similarly to the inductance, the electromagnetic static torque variation is shown in Figure 9 for the same operating point.

The torque variation confirms that the introduction of GOES improves the AFSRM performance. The results show a 7.2% and 11.4% increase of the maximum torque value for, respectively, GOES first and second configuration in comparison with the NOES. Also, the introduction
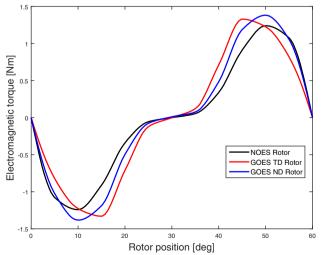

Figure 9: Torque variation with rotor position.

of GOES arranged according to the second configuration (Figure 3) shows a change in the torque waveform in comparison with GOES in the first configuration. This change translates into a shift in the torque peak value which is mainly due to the change in the inductance waveform starting from 10°. However, it is observed that despite the differences in their electromagnetic torque curves, both GOES configurations have relatively close torque mean values (Table 2).

It can be noticed in Figure 9 that the GOES first configuration torque decreases faster than the second configuration due to the inductance slope between 15° and the opposition position (Figure 6). Furthermore, it seems like a short plateau takes shape after reaching a maximum value around 15° and before the decrease, which makes this configuration interesting to exploit the maximum torque. More simulations points might be needed at different current levels in order to confirm the width of the plateau. But since convergence issues have been encountered at the studied current level, it is even more difficult to reach convergence at more saturated current levels.
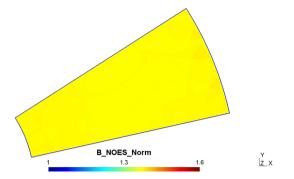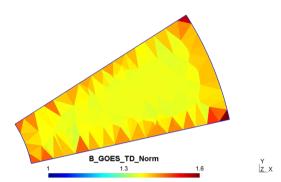

Figure 10: NOES rotor tooth induction levels.

Figure 11: GOES rotor tooth induction levels (configuration # 1).

3.3 Discussion

In order to identify the operating point on the B–H characteristic, an evaluation of the flux density level has been conducted through a simulation for the three studied cases (Figures 10 and 11). The level of flux density noted for NOES case is 1.4 T, which is located in the corresponding B–H knee region (Figure 4).

As far as the GOES case is concerned, an induction level of 1.6 T is found in the rotor tooth. This simulation is given for the alignment rotor position which is representing the highest induction level.

Similarly to the NOES case, the induction levels given in Figures 11 and 12 confirm that the operating point is located in beginning of the knee region of the GOES characteristic given in Figure 4. By taking interest in the induction distribution displayed, a couple of discrepancies can be noticed between the two GOES configurations.

For instance, the highest level of induction in the second configuration is located along the outer and inner radius of the trapezoidal rotor tooth (Figure 12), as opposed to the GOES first configuration in which the highest induction levels are located in the corners (Figure 11).

In the second configuration, both RD and ND are within the same plane which is available to the flux trajectory. Since the flux lines tend to follow the easy magnetization direction (RD), they are less likely to follow a trajectory along the rotor teeth lateral faces. Consequently, this can emphasize a localized saturation as observed in Figure 12.

Table 2: GOES mean and maximum torque increase in comparison with NOES

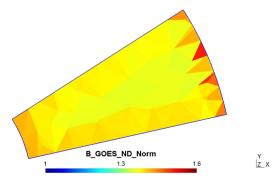| GOES configurations	T_{max} [%]	T_{mean} [%]
GOES first configuration	7.2	16
GOES second configuration	11.4	14.7

Figure 12: GOES rotor tooth induction levels (configuration #2).

For a better understanding of the inductance and electromagnetic variations, an evaluation of the magnetic circuit state at an intermediate (10°) rotor position is given. It is around this rotor position that a change in the inductance slope happens.

It is safe to state that for both GOES configurations, the flux lines tend to mainly follow the easy magnetization direction (RD). However, at the transition from the NOES stator tooth to the GOES rotor tooth, a small deviation can be noticed as the flux favors the TD before quickly aligning with the RD (Figure 10).

On the other hand, in the second configuration the flux lines follow even more strongly the easy magnetization direction since the permeability in the ND is rather small (Figure 4), restricting the flux lines as a result. The local flux lines distribution shown in Figure 13 shows that straight and distinct path is followed in the rotor tooth due to anisotropy which is the sole element influencing the flux path.

Another element that can be assessed and used as an indicator of the AFSRM performance is the torque-per-volume ratios reached for the studied point (Table 3). The results confirm that the use of GOES has a positive impact on the AFSRM performance in comparison with NOES.

It is also worth mentioning that depending on the magnetic state of the circuit, the electromagnetic torque mean value increase can become significant. In previous work [13], the introduction of GOES in a 2D rotating model consistently showed a rise in the torque mean value, which was exacerbated with saturation (an additional 7.6% raise was observed past the knee region).
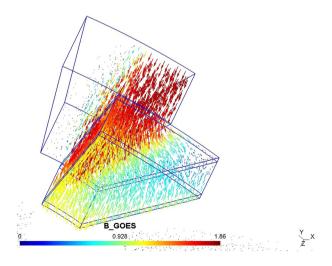
Table 3: Torque-per-volume ratios for the three configurations

Steel case	Torque-per-volume ratio (Nm/m^3)
NOES	1,814
GOES first configuration	2,107
GOES second configuration	2,080

It also showed that the use of GOES in both stator and rotor can improve the electromagnetic torque mean value by an additional 12% in comparison with using it only in the rotor. However, this comes with a consideration for the configuration to be used in the stator. The results presented in the article confirm that the use of GOES in the 3D AFSRM magnetic circuit is beneficial for the machine performance.

4 Conclusion

A performance comparison of a NOES and GOES AFSRM rotor is presented and analyzed in this study. Considering an axial structure where the flux cuts through the rotor, the integration of GOES in the rotor becomes interesting allowing for the steel sheets to be arranged according to two different configurations. In this respect, the introduction of GOES showed steeper inductance slopes in comparison with the NOES case, subsequently leading to an improvement in the electromagnetic torque mean value by up to 16%. One original aspect of our study is the introduction of GOES in an AFSRM, allowing for a compact design along with an interesting torque-to-weight ratio.

Based on these results, future work can include a performance analysis by introducing GOES in the whole magnetic circuit. However, significant convergence issues should be addressed when studying the 3D model as it can be delicate to reach a compromise between convergence and results accuracy for specific rotor positions.

Figure 13: GOES case.

References

[1]   Stephens CM. Fault detection and management system for fault-tolerant switched reluctance motor drives. IEEE Trans Ind Appl. 1991;27(6):1098–102.

[2]   Miller TJE. Optimal design of switched reluctance motors. IEEE Trans Ind Electron. 2002;49(1):15–27.

[3]   Madhavan R, Fernandes BG. Comparative analysis of axial flux srm topologies for electric vehicle application. 2012 IEEE

international conference on power electronics, drives and energy systems (PEDES). Bengaluru, India: IEEE; 2012. p. 1–6.

[4] Tsai J-F, Chen Y-P. Design and performance analysis of an axial-flux disk-type switched reluctance motor for hybrid scooters. JSME Int J Ser C Mech Systems, Mach Elem Manuf. 2006;49(3):882–9.

[5] Murakami S, Goto H, Ichinokura O. A study about optimum stator pole design of axial-gap switched reluctance motor. 2014 International Conference on Electrical Machines (ICEM). Berlin, Germany: IEEE; 2014. p. 975–80.

[6] Labak A, Kar NC. Novel approaches towards leakage flux reduction in axial flux switched reluctance machines. IEEE Trans Magn. 2013;49(8):4738–41.

[7] Xia Z, Kang Y, Wang Q. Developments in the production of grain-oriented electrical steel. J Magn Magn Mater. 2008;320(23):3229–33.

[8] ThyssenKrupp Electrical Steel GmbH. Power Core TM Electrical Steel. ThyssenKrupp Printmedia GmbH, 2011.

[9] Lopez S, Cassoret B, Brudny JF, Lefebvre L, and Vincent JN. Grain oriented steel assembly characterization for the development of high efficiency ac rotating electrical machines. IEEE Trans Magn. 2009;45(10):4161–4.

[10] Demian C, Cassoret B, Brudny J-F, Belgrand T. Ac magnetic circuits using nonsegmented shifted grain oriented electrical steel sheets: Impact on induction machine magnetic noise. IEEE Trans Magn. 2012;48(4):1409–12.

[11] Parent G, Penin R, Lecointe JP, Brudny JF, Belgrand T. Analysis of the magnetic flux distribution in a new shifted non-segmented grain oriented ac motor magnetic circuit. IEEE Trans Magn. 2013;49(5):1977–80.

[12] Ma J, Li J, Fang H, Li Z, Liang Z, Fu Z, et al. Optimal design of an axial-flux switched reluctance motor with grain-oriented electrical steel. IEEE Trans Ind Appl. 2017;53(6):5327–37.

[13] Sugawara Y, Akatsu K. Characteristics of a switched reluctance motor using grain-oriented electric steel sheet. 2013 IEEE ECCE Asia Downunder. Melbourne, Australia: IEEE; 2013. p. 1105–10.

[14] Kaneki O, Higuchi T, Yokoi Y, Abe T, Miyamoto Y, Ohto M. Performance of segment type switched reluctance motor using grain-oriented. 2012 15th International Conference on Electrical Machines and Systems (ICEMS). IEEE; 2012. p. 1–4.

[15] Belhadi M-H, Krebs G, Marchand C, Hannoun H, Mininger X. Evaluation of axial srm for electric vehicle application. Electr Power Syst Res. 2017;148:155–61.

[16] Aydoun R, Parent G, Lecointe J-P, Tounzi A. Investigating the use of grain-oriented electrical steel in axial-flux switched reluctance machines. Int J Appl Electromagnetics Mechanics. 2020;63(4):691–703. doi: 10.3233/JAE-209205.

[17] Hihat N, Lecointe J-Ph, Ninet O, Duchesne S, Napieralska E, Wiak S. Normal permeability of grain non-oriented, grain oriented and amorphous electrical steel sheets. Int J Appl Electromag Mech. 2014;46(2):349–54.